Isotype-specific Selection of High Affinity Memory B Cells in Nasal-associated Lymphoid Tissue

Michiko Shimoda,[1] Toru Nakamura,[2] Yoshimasa Takahashi,[2] Hideki Asanuma,[3] Shin-ichi Tamura,[3] Takeshi Kurata,[3] Tsuguo Mizuochi,[4] Norihiro Azuma,[1] Choemon Kanno,[1] and Toshitada Takemori[2]

[1]*Department of Applied Biochemistry, Utsunomiya University, Tochigi 321-8505, Japan*
[2]*Department of Immunology and the* [3]*Department of Pathology, National Institute of Infectious Diseases, Tokyo 162-8640, Japan*
[4]*Laboratory of Biomedical Research, Department of Applied Biochemistry, Tokai University, Kanagawa 259-1292, Japan*

Abstract

Mucosal immunoglobulin (Ig)A dominance has been proposed to be associated with preferential class switch recombination (CSR) to the IgA heavy chain constant region, *Cα*. Here, we report that B cell activation in nasal-associated lymphoid tissue (NALT) upon stimulation with the hapten (4-hydroxy-3-nitrophenyl)acetyl (NP) coupled to chicken γ globulin caused an anti-NP memory response dominated by high affinity IgA antibodies. In the response, however, NP-specific IgG^+ B cells expanded and sustained their number as a major population in germinal centers (GCs), supporting the view that CSR to IgG heavy chain constant region, *Cγ*, operated efficiently in NALT. Both IgG^+ and IgA^+ GC B cells accumulated somatic mutations, indicative of affinity maturation to a similar extent, suggesting that both types of cell were equally selected by antigen. Despite the selection in GCs, high affinity NP-specific B cells were barely detected in the IgG memory compartment, whereas such cells dominated the IgA memory compartment. Taken together with the analysis of the V_H gene clonotype in GC and memory B cells, we propose that NALT is equipped with a unique machinery providing IgA-specific enrichment of high affinity cells into the memory compartment, facilitating immunity with high affinity and noninflammatory secretory antibodies.

Key words: memory • affinity maturation • germinal center • IgA • NALT

Introduction

Mucosal surfaces are exposed to pathogenic organisms and foreign antigens, and are thus major sites for the start of infection and inflammation. M cells in the follicular epithelial layer of the mucosa-associated lymphoid tissues (MALTs)* transcytose the pathogenic organisms and foreign antigens to underlying APCs (for reviews, see references 1–3). APCs process antigens and stimulate antigen-specific $CD4^+$ Th cells in MALT, which, in turn, results in activation of B cells (1–3). The mucosal B cell response is dominated by IgA antibody production, a feature strikingly different from that in peripheral lymphoid organs (1–3). Consequently, mucosal surfaces are covered with secretions containing large amounts of secretory IgA that plays a critical role in facilitating defense against exposure to numerous environmental antigens (4). Mucosal IgA dominance is considered to reflect a preferential class switch recombination (CSR) from μ to α (5), through stimulation with TGF-β, IL-10, and CD40 (6–9); however, the mechanism of this process in vivo is not fully understood.

Analysis of the nonmucosal immune system indicates that, in response to T cell–dependent antigens, B cells are activated by interaction with T cells and form germinal centers (GCs) (10, 11). The cellular volume of spleen GC

H. Asanuma's current address is Department of Applied Biochemistry, School of Engineering, Tokai University, Kanagawa 259-1292, Japan.

Address correspondence to Toshitada Takemori, Dept. of Immunology, National Institute of Infectious Diseases, 1-23-1 Toyama, Shinjuku-ku, Tokyo 162-8640, Japan. Phone: 03-5285-1111 ext. 2102; Fax: 03-5285-1156; E-mail: ttoshi@nih.go.jp

**Abbreviations used in this paper:* ASC, antibody-secreting cell; CSR, class switch recombination; CT, cholera toxin; GC, germinal center; i.n., intranasal; MALT, mucosa-associated lymphoid tissue; NALT, nasal-associated lymphoid tissue; NIP, (4-hydroxy-5-indo-3-nitrophenyl)acetyl; NP, 4-hydroxy-3-nitrophenyl)acetyl; PCLN, posterior cervical LN; PI, propidium iodide; PNA, peanut agglutinin; RAG, recombination activating gene.

peaks at 2 wk after immunization, followed by a reduction toward the basal level by days 80–100 (12, 13). Concomitantly, long-lived antibody-secreting cells (ASCs) and memory B cells start to appear ~1–2 wk after immunization, and they persist largely without proliferation (14–19). GCs support a specialized environment for CSR and antigen-driven somatic hypermutation, which randomly diversifies the antibody repertoire (20, 21). The accumulation of somatic mutations increases the antibody affinity for eliciting antigen, but it might also change the antibody specificity, sometimes resulting in the acquisition of autoreactivity (22). High affinity B cells selectively receive appropriate signals through interaction with follicular dendritic cells and GC Th cells to differentiate into memory B cells (11, 23). Genetic analysis of B cells in human tonsils suggested that somatic mutation, CSR, and, presumably, selection for antigen also take place in GCs in MALT (24, 25). To date, however, it remains largely unknown how the antigen-specific repertoire is selected and reserved in the mucosal memory compartment, because of technical difficulties in the genetic and cellular analysis of the mucosal B cell response to defined antigens at the clonal level.

Nasal-associated lymphoid tissue (NALT) is the major inductive site for the upper respiratory tract and oral cavity (for reviews, see references 26 and 27), equivalent to Waldeyer's ring in humans, consisting of sites such as adenoids or tonsils (26). NALT is located in close proximity to sites of entry by foreign antigens and infectious agents, and intranasally delivered antigens are taken up from the nasal cavity preferentially through M cells (26). Thus, NALT is easily manipulated by intranasal (i.n.) inoculation of antigen (28, 29), providing a useful experimental system for analyzing antigen-driven selection in GCs and the subsequent establishment of a memory compartment in the mucosal immune system.

To investigate antigen-driven selection in NALT GCs and its role in the establishment of the memory compartment, we took advantage of the genetically highly restricted immune response of C57BL/6 mice to the hapten (4-hydroxy-3-nitrophenyl)acetyl (NP). In the primary response to NP, the majority of the NP-specific B cells express antibodies encoded by a canonical V_H gene, *V186.2*, paired with λ1 light chain (30, 31). Affinity-driven selection results in the enrichment of *V186.2* joined to *DFL16.1* and J_H2 segments carrying an affinity-enhancing replacement mutation from tryptophan to leucine at amino acid position 33 (Trp33 to Leu33), first within the GC B cell compartment (31–34) and later within the memory compartment (19, 32, 35). By using these genetic and phenotypic markers, we were able to track a very small population of NP-specific GC and memory B cells in the mucosal lymphoid tissues.

In this study, we demonstrate that high affinity B cells were preferentially enriched in the IgA memory compartment in the primary immune response in NALT, despite the equivalent generation and selection of high affinity B cells within both the IgG^+ and IgA^+ GC compartments. The present data further suggest that high affinity memory B cells not only home back to regional mucosa but also migrate into nonmucosal tissues to establish a long-term memory compartment predominant in IgA.

Materials and Methods

Animals and Immunizations. Specific pathogen-free female C57BL/6 mice and recombination activating gene (RAG)-$1^{-/-}$ mice were purchased from Japan SLC Inc. and The Jackson Laboratory, respectively. Mice 10–12 wk of age were given an i.n. challenge into each nasal cavity with 3 μl of PBS containing 1 μg of NP_{16}-CG and 1 μg of cholera toxin (CT; Sigma-Aldrich). As a control, mice were given an intraperitoneal challenge of 2 μg of NP_{16}-CG and 2 μg of CT. Some mice received a secondary challenge of soluble NP_{16}-CG (2 μg i.n. or 20 μg intraperitoneally) 5 or 7 wk after the primary sensitization. All mice were maintained under specific pathogen-free conditions in accordance with institutional animal care and use guidelines.

Preparation of Nasal and Intestinal Secretions. To collect nasal secretions, we separated the upper and lower jaws, and the nasal draining duct to the oral cavity was exposed. The nasal cavity was flushed with 1 ml of 0.1% BSA in PBS, and the washing was recycled to flush the cavity three times. To collect intestinal secretions, we cut open a piece of small intestine (~6 cm in length) and rinsed it with 0.1% BSA in PBS with 0.05% sodium azide to wash out the ingredients. The piece was placed in a fresh dish containing 2 ml of 0.1% BSA in PBS with 0.05% sodium azide, and mucosal secretion was scraped from the intestinal lumen with the plunger of a syringe. The solution containing nasal or intestinal secretions was centrifuged (15,000 rpm) at 4°C for 10 min, and the supernatant was recovered for analysis.

Cell Preparations. NALT localized on the posterior part of the palate were gently teased out with fine forceps and single cell suspensions prepared by filtering through nylon mesh (28, 29). Posterior cervical LNs (PCLNs) were identified deep within the musculature of the neck and excised (36). Single-cell suspensions were prepared from PCLNs and spleens by mechanical disruption of small fragments of organ between frosted glass slides followed by filtration through nylon mesh. RBCs were then lysed as described previously (34).

Cell Transfer. Spleen cells were prepared from C57BL/6 mice as >4 wk after i.n. immunization with 2 μg of CT adjuvant and 2 μg of either NP_{16}-CG or CG. Cells were then transferred into RAG-$1^{-/-}$ mice on a C57BL/6 background by intravenous injection (6×10^7 cells per recipient). 12–24 h after the transfer, the RAG-$1^{-/-}$ mice were challenged intraperitoneally with 50 μg of soluble NP_{16}-CG. 7 d later, mice were individually bled and the serum used for ELISA (see below).

Flow Cytometry. Single cell suspensions of NALTs, PCLNs, and spleens were blocked with anti-FcγRII/III mAb (2.4G2) on ice for 30 min. GC B cells and memory B cells were identified as reported previously (12, 19, 37). Briefly, to analyze the kinetics of IgA^+ or $IgG2b^+$ GC and memory cells, we incubated cells with TexasRed-conjugated anti-CD38 ($CD38^{TX}$), FITC-labeled anti-λ1, and anti-λ2 mAbs (anti-λ^{FITC}, Ls-136 and 4/1–101), PE-conjugated (4-hydroxy-5-indo-3-nitrophenyl)acetyl (NIP)-BSA ($NIP\text{-}BSA^{PE}$), and with biotinylated anti-IgA or anti-IgG2b mAb, respectively (BD PharMingen). Secondary incubation was with APC-conjugated streptavidin ($streptavidin^{APC}$; BD PharMingen). To analyze NP-specific/λ^+ GC and memory B cells, cells were stained with a mixture of biotinylated mAbs against IgM, IgD, CD43, CD5, and CD90 to exclude naive B cells, anti-

body-forming cells (AFCs), B-1 cells, and T cells from the analysis, as described previously (19). After washing, cells were stained with anti-CD38^{TX}, APC-conjugated anti-B220 (B220^{APC}), and anti-λ^{FITC} mAbs and with NIP-BSA^{PE}, followed by staining with Tricolor (TC)-conjugated streptavidin (streptavidin^{TC}; Caltag). The cells were washed and finally suspended in 5 μg/ml of propidium iodide (PI) for analysis with a FACSVantage™ (Becton Dickinson) as described previously (34). At least 100,000 events were collected, and the frequency of NIP-binding GC and memory cells in the viable lymphocyte gate was determined with CELLQuest™ (version X; Becton Dickinson). To sort GC and memory B cells in NALTs or PCLNs, we obtained cells from pooled NALTs (n = 80–100) or pooled PCLNs (n = 10–30). Cells were blocked with 2.4G2 and stained with biotinylated mAbs against IgM, IgD, CD43, CD5, and CD90. After washing, cells were stained with NIP-BSA^{PE} and anti-λ^{FITC}, anti-CD38^{TX} and anti-B220^{APC} mAbs, followed by streptavidin^{TC} and PI as reported previously (19). PI-stained dead cells, IgM$^+$, IgD$^+$, CD43$^+$, CD5$^+$, and CD90$^+$ cells were excluded by gating and NIP-binding/B220$^+$/CD38^{dull}/λ$^+$ GC B cells and NIP-binding/B220$^+$/CD38$^+$/λ$^+$ memory cells (12, 19, 37) were sorted with a FACSVantage™ directly into Trizol (GIBCO BRL) containing 50 μg/ml tRNA (Roche Diagnostics). As a control, NIP-binding/B220$^+$/CD38^{dull}/λ$^+$ GC B cells were sorted from splenocytes of C57BL/6 mice (n = 3) immunized intraperitoneally with 2 μg of NP-CG and 2 μg of CT 9 d earlier.

ELISA and ELISPOT Assays. ELISA and ELISPOT assays were performed with NP_1-BSA and NP_{22}-BSA as described previously (35). The frequency of NP-specific AFCs was estimated among NALT cells, splenocytes, and bone marrow cells, and total and high affinity NP-specific antibodies were determined in sera. The quantity of each subclass of NP-specific antibody was measured with biotinylated goat anti–mouse IgG1 (Biosource International), IgG2b (Biosource International), IgA (Zymed Laboratories), or biotinylated anti-λ antibodies (Southern Biotechnology Associates, Inc.), and with streptavidin-conjugated horseradish-peroxidase (Roche Molecular Biochemicals) by use of an isotype-specific standard curve that was constructed in each assay based on serial dilutions of purified anti-NP λ$^+$ mAb of the IgG1 and IgG2b subclass (provided by T. Azuma, RIBS, Science University of Tokyo, Tokyo, Japan). For measurement of NP-specific IgA antibodies, pooled sera from hyperimmune mice containing NP-specific IgA antibodies equivalent to 640,000 U were used as standards, and the quantity was determined as relative IgA units.

Sequence Analysis of VDJ DNA Segments. Total RNA was prepared from sorted Trizol-solubilized NALT, PCLNs, or splenic λ$^+$ GC B cells and memory B cells based on the manufacturer's protocol. First-strand cDNA was synthesized with specific primers, Cγ 5-GTGT/CGCACACC/TG/ACTGGACAGGGA/CTCCAG/TAG, Cα 5-CAGCGGCCGCGGCAGCTGGGA, Cμ 5-GCCAGGCAGCCCATGGCCACC, or with an oligo-dT primer by use of a Superscript Kit (GIBCO BRL). The Cγ–specific primer was designed so that all the subclasses of γ rearrangements (γ1, γ2a, γ2b, and γ3) would be primed. The latter was confirmed in preliminary experiments with cDNA prepared from both NP-specific hybridoma clones of each IgG subclass encoded by *V186.2* gene rearrangements (provided by T. Azuma), and spleen cells of mice immunized intraperitoneally with alum-precipitated NP-CG.

2 μl of cDNA solution was used as a template in a reaction volume of 50 μl for two rounds of nested PCR for amplifying the *V186.2* gene rearranged to the Cγ or Cα region by use of *Pfu* DNA polymerase (Stratagene). The primers used for the nested PCR were as follows: as a sense-primer, *V186.2*-specific primers were used (35); as an antisense primer, Cγ 5-CAGGGGC-CAGTGGATAGACAGATG, Cα 5-GTGAATTCAGGCG-GCCGCTTA, or Cμ 5-AGGGGGCTCTCGCAGGAGACG was used. PCR products were size-fractionated by agarose gel electrophoresis and purified with GFX™ PCR DNA and a Gel Band Purification kit (Amersham Pharmacia Biotech). The purified fragments were cloned into the PCR-Script™ Amp cloning vector (Stratagene) according to the manufacturer's instructions. The three independent RT-PCR and ligation reactions were performed and were pooled to create each cDNA library to minimize the bias from PCR amplification. At least 20 independent bacterial Amp^r white colonies with insert were sequenced. The sequence of the *VDJ* segment in a plasmid vector was determined with an ABI PRIZM™ Big-Dye Terminator Cycle Sequencing system (310 Genetic Analyzer; Cetus/Perkin-Elmer). Assignment of gene usage and somatic mutations was performed with the BLAST and CLUSTALW programs provided by the DDBJ (www.ddbj.nig.ac.jp). Redundant sequences were deleted on the assumption that such clones were derived from a single gene. To estimate the error mutation-frequency of our RT-PCR cloning system, germline *V186.2* gene rearrangements were amplified from total RNA of a NP-specific hybridoma, B1–8 (30, 38), and 28 bacterial Amp^r colonies were sequenced. The artificial mutation-frequency was estimated to be $1.2 10^{-4}$ base pair (one substitution in 8,232 nucleotides), implying 0.04 mutations per *V186.2* gene.

Statistical Analysis. Fisher's exact test and the Mann-Whitney nonparametric (two-tailed) test were used with Abacus Concepts, StatView (Abacus Concepts, Inc.). A $P < 0.05$ was considered to indicate a significant difference.

Results and Discussion

I.N. Immunization Causes Rapid Expansion of IgA and IgG2b GC B Cells in NALT. To investigate the dynamics and affinity maturation of IgG$^+$ and IgA$^+$ B cells in the primary response to NP in NALT, we immunized C57BL/6 mice intranasally with NP-CG in the presence of CT adjuvant and monitored NP-specific B cells in NALT by flow cytometry with use of the hapten NIP coupled to BSA as described previously (34). Since preliminary experiments had suggested that IgG2b was the major fraction of the total IgG response in NALT (data not shown and see Table I), we monitored NIP-binding IgG2b$^+$ cells as representative of IgG$^+$ B cells.

As shown in Fig. 1 A panel c, intraperitoneal immunization with NP-CG and CT induced a rapid expansion of NIP-binding/CD38^{dull}/B220$^+$ and CD38^{dull}/B220^{dull} cells in the spleen at day 9 after immunization. CD38^{dull}/B220^{dull} B cells are defined as plasmablasts and AFCs (39) while CD38^{dull}/B220$^+$ cells bound high levels of peanut agglutinin (PNA) (Fig. 1 A panel e), a feature characteristic of GC B cells (40). As shown in Fig. 1 A panel d, i.n. inoculation with NP-CG and CT caused a rapid expansion of NIP-binding B cells in a B220$^+$/CD38^{dull} population in NALT at day 7 after immunization, ~40-fold above the level of nonimmunized mice. The majority of NIP-binding B cells displayed the phenotype of GC B cells (B220$^+$/

Table I. *Summary of λ+/NIP-binding B Cells with GC (CD38dull) or Memory (CD38+) Phenotype*[a]

			IgG1/2a/2b	Y99/DFL16.1			L33/Y99		
	Day	Class	%[b]	%[b]	*P* value[c]		%[b]	*P* value[c]	
SPLGC	9	IgG	90/5/5	21			<5.2 (0/19)		
NALT	9	IgG	5/10/85	50		0.0823[d]	<5.2 (0/20)		0.0116[d]
GC		IgA		48	>0.9999		21.7 (5/23)	0.0511	
	11	IgG	6/19/75[f]	88			31.2 (5/16)		
		IgA		43	0.0332		<10.0 (0/11)	0.0598	
	13	IgG	3/23/74[f]	45		0.0159[d]	3.2 (1/31)		0.0134[d]
		IgA		68	0.1098		8.0 (2/25)	0.5806	
NALT	11	IgG	0/80/20[f]	20		0.0034[g]	<10.0 (0/10)		
Memory		IgA		70	0.0698		<10.0 (0/10)	>0.9999	
	13	IgG	8/67/25[f]	33		0.0177[g]	<8.3 (0/12)		
		IgA		55	0.4136		<9.1 (0/11)	>0.9999	
PCLNs	11	IgG	20/10/70	30			<10.0 (0/10)		
GC		IgA		62	>0.9999		<12.5 (0/8)	>0.9999	
	13	IgG	27/9/64	37			27.3 (3/11)		
		IgA		33	>0.9999		<16.7 (0/6)	0.5147	
	15	IgG	9/27/64	27			<9.1 (0/11)		
		IgA		90	0.0075		<10.0 (0/10)	>0.9999	
PCLNs	11	IgG	0/21/79	33			<4.2 (0/24)		
Memory		IgA		71	0.0278		<5.9 (0/17)	>0.9999	
	13	IgG	11/18/71	7			<3.6 (0/28)		
		IgA		80	>0.0001		45.0 (9/20)	0.0001	0.0015[e]
	15	IgG	16/16/68	35			<5.3 (0/19)		
		IgA		86	0.0261		42.9 (3/7)	0.0135	0.0173[e]

[a]The sequence data are depicted in Fig. 2 except for those of IgG clones of splenic GC at day 9 after immunization. These sequence data are available from GenBank/EMBL/DDBJ under accession nos. AB057817-AB058198 and AB067398-AB067440.
[b]The percentage was calculated as 100× (number of V186.2 clones with each phenotype/number of V186.2 clones).
[c]The Fisher's *P* value between the value for IgG and IgA clones at the indicated date after immunization unless noted otherwise.
[d]The Fisher's *P* value between the value for IgG clones at day 11 and the indicated date after immunization.
[e]The Fisher's *P* value between the value for IgA clones at day 11 and the indicated date after immunization.
[f]The Fisher's $P < 0.0138$ between the value for IgG2a/IgG2b clones from NALT B cells with GC and memory phenotype at each indicated date after immunization.
[g]The Fisher's *P* value between the value for IgG clones of NALT GC at day 11 and of NALT memory at the indicated date after immunization.

PNA^+), whereas NIP-binding B cells with the phenotype of plasmablasts and AFCs were much less frequent in NALT from days 6 to 15 after immunization (Fig. 1 A panels d and f, and data not shown), probably owing to their migration from NALT into the epithelial layer immediately after differentiation (references 41 and 42 and see below). Consistent with this, ELISPOT analysis showed that NIP-binding/λ^+ ASCs were barely detected (≤4 out of 10^5 mononucleated cells) in NALT from days 7 to 11 after immunization (data not shown).

We analyzed the kinetics of NP-specific GC B cells in NALT (Fig. 1 B and data not shown) by five-color flow cytometry (references 19 and 34 and see Materials and Methods). As shown in Fig. 1 B, the frequency of GC B cells reached a maximum at day 7 and was sustained up to day 11 after immunization in the immunized mice (n = 80–100 per group) and reduced toward the basal level from days 13 to 15 after immunization. NIP-binding/λ^+ GC B cells bearing IgG2b and IgA coordinately appeared in NALT after inoculation with NP-CG and CT; $IgG2b^+$ cells were the major population ~3–4 times the number of IgA^+ cells, except at day 9 after immunization. In contrast, intraperitoneal immunization with NP-CG and CT caused an expansion of NIP-binding $IgG1^+$ GC B cells in the spleen, which dominated over $IgG2b^+$ cells (data not shown and Table I). These results suggest that CSR from $C\mu$ to $C\gamma 2b$ occurred efficiently in B cells in NALT upon stimulation with NP-CG and CT.

IgA and IgG GC B Cells Are Equally Mutated and Selected by Antigens in NALT. Accumulation of somatic mutations within GCs increases antibody affinity for eliciting antigen, and the subsequent clonal selection allows a selec-

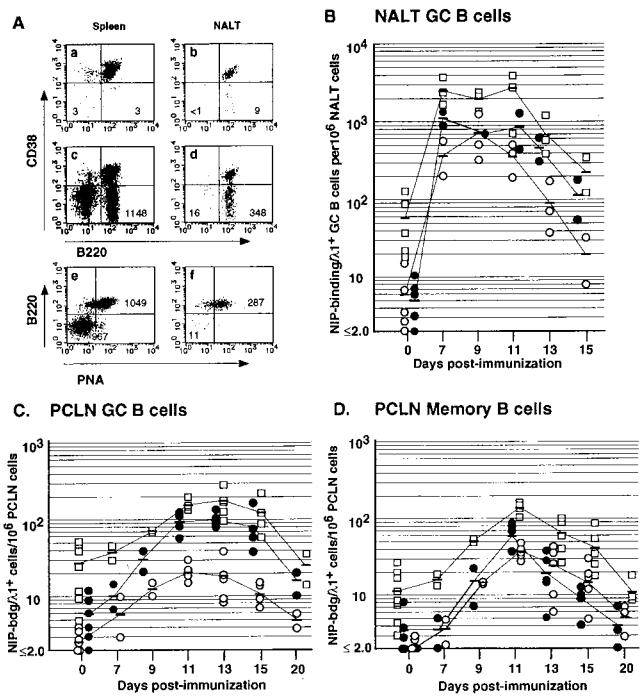

Figure 1. Flow cytometric analysis of NP-specific B cells. (A) Spleen cells were obtained from both nonimmunized C57BL/6 mice (panel a) and mice immunized intraperitoneally with 2 μg of NP-CG and 2 μg of CT 9 d earlier (panels c and e). Pooled NALT cells (n = 20–25 mice) were also obtained from nonimmunized C57BL/6 mice (panel b) as well as from mice immunized i.n. with 2 μg of NP-CG and 2 μg of CT 7 d earlier (panels d and f). Cells were stained with anti-$B220^{TX}$ and anti-$CD38^{APC}$ mAbs and with NIP-BSA^{PE}, PNA^{FITC}, and PI. Viable cells (PI^-) were selected under a lymphocyte gate based on forward and side light scatter. Thereafter, the NIP-binding cells were gated, and the expression of B220 and CD38 was analyzed (panels c and d). Finally, the $CD38^{dull}$ population was gated, and binding to PNA was analyzed among the NIP-binding cells (panels e and f). Figures in each region represent the number of $CD38^{dull}$/NIP-binding/$B220^+$ or $B220^{dull}$ cells (panels a–d) and that of $CD38^{dull}$/NIP-binding/$B220^+$/PNA^+ or $CD38^{dull}$/NIP-binding/$B220^{dull}$/PNA^- cells (panels e and f) per 100,000 total viable cells. (B–D) Cells were prepared from pooled NALT (B, n = 20–25 mice) and PCLNs (C and D, n = 5–20) at various times after i.n. immunization (as above) as well as from nonimmunized mice. To monitor NP-specific/λ^+ GC and memory B cells, cells were first stained with biotinylated mAbs against IgM, IgD, CD43, CD5, and CD90. This was followed by staining with NIP-BSA^{PE} and anti-$CD38^{TX}$, anti-λ^{FITC}, and anti-$B220^{APC}$ mAbs. After washing, cells were stained with $streptavidin^{TC}$ and PI to exclude from the analysis dead cells and the cells recognized by the biotinylated mAbs. To track NP-specific/λ^+ IgA^+ or $IgG2b^+$ GC and memory B cells, cells were stained with anti-$CD38^{TX}$ mAb, anti-λ^{FITC} mAb, NIP-BSA^{PE}, and with biotinylated anti-IgA or IgG2b mAb, followed by incubation with APC-conjugated streptavidin and PI. Viable cells were selected under a lymphocyte gate based on forward and side light scatter. Shown are the frequencies of NIP-binding/λ^+ GC B cells (□) and NIP-binding/λ^+ $IgG2b^+$ (●) or IgA^+ (○) GC B cells in NALT (B) and PCLNs (C). Also shown are the frequencies of NIP-binding/λ^+ memory B cells (□) and NIP-binding/λ^+ $IgG2b^+$ (●) or IgA^+ (○) memory B cells in PCLN (D). Each symbol represents the result from a single experiment. Frequency was estimated by dividing the number of cells with each phenotype by the total number of viable cells. At least 10^5 events were collected for each frequency determination.

tive accumulation of high affinity variants which preferentially differentiate into long-term ASCs and memory cells (11, 23). To examine whether somatic mutation and antigen-driven selection operate equally well in IgG^+ and IgA^+ GC B cells in NALT in the primary response to NP, we purified NIP-binding/λ^+ GC B cells with a phenotype of $CD38^{dull}$/$B220^+$/IgM^-/IgD^-/$CD43^-$/$CD5^-$/$CD90^-$ from the pooled NALTs of 80–100 C57BL/6 mice at indicated periods after i.n. inoculation with NP-CG and CT. As a control, NP-specific GC B cells were purified from the pooled spleens of C57BL/6 mice immunized intraperitoneally with NP-CG and CT 9 d previously.

In C57BL/6 mice, the anti-NP antibody response to T cell–dependent antigen is dominated by $\lambda1^+$ antibodies whose H-chain variable (V) region is encoded by the V segment, *V186.2* (31, 43, 44). In contrast, the predominant usage of the rearranged *V186.2* gene is barely detected in T cell–independent responses (45). Thus, first strand cDNA was synthesized from total RNA of purified cells by use of either a *Cμ*, *Cγ*, or *Cα* specific primer or oligo-d(T) primer, followed by two rounds of nested PCR for preferential amplification of the V_H gene belonging to the *V186.2* or *V3* subfamily (35). Subsequently, we sequenced the amplified *VDJ* clones to identify the V_H gene usage and any mutations present (Table I and Fig. 2).

We observed that >90% of the V_H genes recovered from NALT GC were encoded by the *V186.2* gene segment, except for the genes isolated at day 11 after immunization (40% of the recovered V_H genes). As summarized in Table I, among the *VDJ-Cγ* clones sequenced, the rearranged *V186.2* genes joined to *Cγ2b* (*VDJ-Cγ2b*) were dominant throughout the primary immune response (71–85%). In contrast, 90% of the total *VDJ-Cγ* clones were joined to *Cγ1* in GC B cells in the spleens of mice immunized intraperitoneally with NP-CG and CT at day 9 after immunization. Rearranged *V186.2* genes joined to *Cα* (*VDJ-Cα*) were not recovered from the spleens of these mice.

As shown in Fig. 2 A and B, NP-specific GC B cells bearing either IgG or IgA accumulated somatic mutations in the rearranged *V186.2* genes as early as at day 7 after immunization. The average number of mutations per rearranged *V186.2* gene increased from days 7 to 11 after immunization in the *VDJ-Cγ* (from 0.9 to 3.7; Fig. 2 A) and *VDJ-Cα* clones (from 0.8 to 3.1; Fig. 2 B), accompanying the reduction in the frequency of *V186.2* clones with one or no mutation. These results suggest that both IgG^+ and IgA^+ GC B cells in NALT proliferated and accumulated somatic mutations at a similar rate in the rearranged *V186.2* genes in the primary immune response. The average number of mutations per rearranged *V186.2* gene, however, became less frequent from days 11 to 13 after immunization (from 3.7 to 1.8 in *VDJ-Cγ* and from 3.1 to 2.0 in *VDJ-Cα*) in parallel with the reduction in cell number. This may reflect preferential egression of the mutated cells from GC (Fig. 2 A and B).

Antigen-driven clonal selection in C57BL/6 mice in response to NP-CG causes the predominant selection of NP-specific/λ^+ antibodies encoded by the *V186.2* gene rearranged to *DFL16.1* and J_H2 segments carrying a tyrosine residue at position 99 in CDR3 and a replacement mutation from tryptophan (Trp) to leucine (Leu) at position 33 in CDR1 (the Leu33/Tyr99 group). The Leu33 substitu-

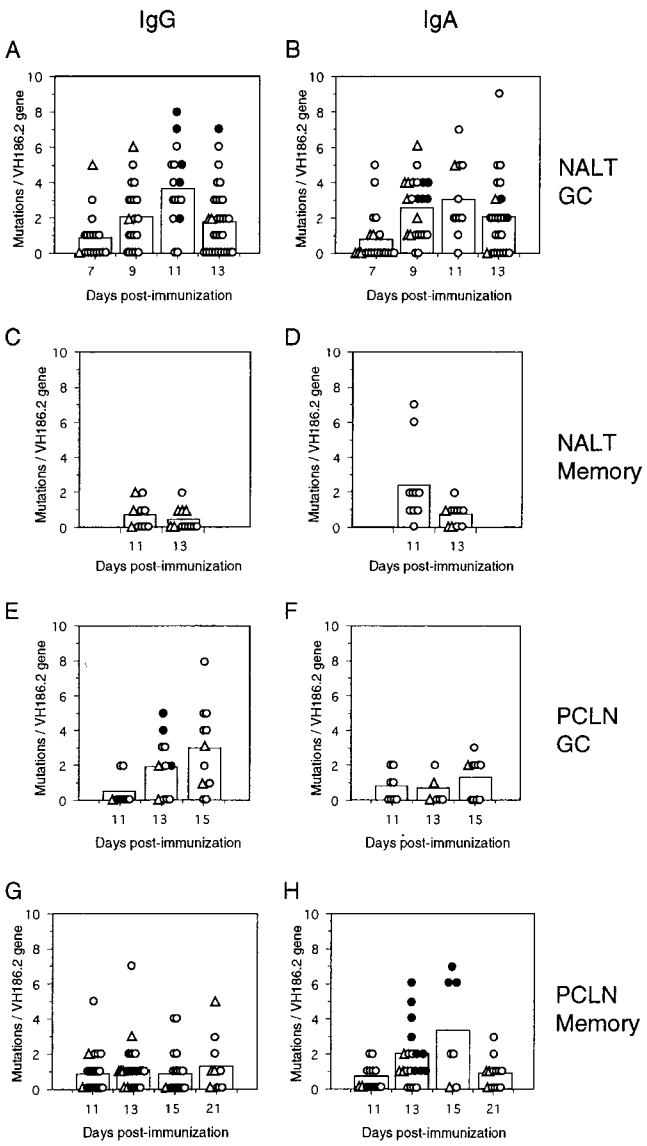

Figure 2. Accumulation of somatic mutations and affinity maturation in NP-specific GC B cells (A, B, E, F) and memory B cells (C, D, G, H) in NALTs (A–D) and PCLNs (E–H) of C57BL/6 mice after i.n. immunization with NP-CG and adjuvant CT. NIP-binding/λ^+ GC B cells ($CD38^{dull}/B220^+/IgM^-/IgD^-/CD43^-/CD5^-/CD90^-$) and NIP binding/$\lambda^+$ memory B cells ($CD38^+/B220^+/IgM^-/IgD^-/CD43^-/$ $CD5^-/CD90^-$) were purified from the pooled NALTs (n = 80–100) or PCLNs (n = 10–30) of NP-CG primed C57BL/6 mice at various times after immunization. Messenger RNA was purified from sorted cells, and cDNA synthesized by reverse transcriptase with specific primers for either Cγ (A, C, E, G) or Cα (B, D, F, H). Thereafter, the rearranged V_H genes were amplified from the cDNA by PCR. The frequency of artificial substitutions was calculated to be $1.2 10^{-4}$ base pair in control experiments using messenger RNA from the hybridoma B1–8 (see Materials and Methods). V_H genes encoded by *V186.2* were dominant among the recovered clones and were selected for further analysis (see Table I). Shown are the numbers of somatic mutations in individual *V186.2* genes with (●) or without (○) a Trp-to-Leu substitution at position 33 (Leu33) and genes with Gly at amino acid 99 in CDR3 (△) recovered at the indicated date. The average number of somatic mutations of *V186.2* genes (white columns) at the indicated date was determined by dividing the total number of somatic mutations observed by the number of clones. The sequence data are available from GenBank/EMBL/DDBJ under accession nos. AB057817-AB058198 and AB067398-AB067440.

tion usually yield ~10-fold increase in affinity for NP in antibodies from primary and secondary NP-specific ASCs (31, 44, 46) and NP-specific GC B cells (unpublished data). In this context, as shown in Fig. 2 and Table I, the Leu33/Tyr99 group was transiently selected in 22% of the *VDJ-Cα* clones from NALT GC B cells at day 9 after immunization ($P = 0.0511$), but this selection was not apparent in the *VDJ-Cγ* clones at that period. From days 9 to 11 after immunization, the *VDJ-Cγ* clones increased the R/S ratio in CDR1 and CDR2 above the value expected in random mutations ($P = 0.0109$, data not shown) and enriched the Leu33/Tyr99 group (31%, $P = 0.0116$); however, the Leu33/Tyr99 group became less frequent from days 11 to 13 after immunization ($P = 0.0134$). These results suggest that the *VDJ-Cγ* clones were highly selected by antigen at day 11 after immunization, but the selection was transient.

It has been suggested that antigen-driven clonal selection at a later stage of the primary response results in the enrichment of high affinity anti-NP antibodies encoded by *V_H186.2-D-J* gene segments with glycine at position 99 in CDR3 (the Tyr33/Gly99 group), in association with a number of somatic mutations except for the Leu33 replacement (19, 44). The Tyr33/Gly99 group appeared in the *VDJ-Cγ* and *VDJ-Cα* clones in NALT GC at a low frequency, accompanied by a small number of mutations (Fig. 2 A and B), compatible with the view that these clones are not selected in NALT B cells during the early primary response, as expected (19, 44).

Taken together, these results support the notion that introduction of somatic mutations and subsequent antigen-driven selection operates equally well in both NP-specific IgA^+ and IgG^+ GC B cells in NALT after i.n. inoculation with NP-CG and CT.

Memory B Cells Are Barely Detected in NALTs after Immunization but Appear in the Draining LNs, PCLNs. We have previously observed that NP-specific $IgG1^+$ memory cells were enriched in $IgM^-/IgD^-/CD38^+$ B cells in the spleen of C57BL/6 mice after intraperitoneal immunization with NP-CG in alum (19). Memory B cells appeared behind the peak response of GC and reached a plateau at a frequency of $1–2 \times 10^{-4}$ per mononucleated spleen cell, 10–20 times below the peak level of GC B cells (12, 19). In NALT, however, we observed that the frequency of $IgG2b^+$ and IgA^+ B cells with a memory phenotype was low, >100 times below the level of GC B cells ($<10^{-5}$ per mononucleated cell; data not shown). NALT are constituted bilaterally of two separate organs (26–28) that contain $2–4 \times 10^5$ mononucleated cells in immunized C57BL/6 mice (data not shown), implying that NALT could retain only 2–4 memory cells during the immune response, if any. Nevertheless, to examine B cell selection in the memory compartment, NIP-binding/λ^+ B cells with a memory phenotype ($B220^+/CD38^+/IgM^-/IgD^-/$ $CD43^-/CD5^-/CD90^-$) were purified from pooled NALTs (n = 85–100) at days 11 and 13 after immunization and subjected to PCR that amplifies *VDJ-Cγ* and *VDJ-Cα* clones. The sequence analysis revealed that, unlike the *VDJ-Cγ* clones of NALT GC B cells, clones from

memory B cells taken at days 11 and 13 after immunization were dominated by the *V186.2* gene segment with one or no mutation joined to *Cγ2α* (Fig. 2 C and Table I). Likewise, as shown in Fig. 2 D, eight out of ten *VDJ-Cα* clones sequenced had a low number of mutations at day 11 after immunization and the average number of mutations per *VDJ-Cα* gene reduced from 2.4 to 0.7 at day 13 immunization. Furthermore, in contrast to NALT GC B cells, the Leu33/Tyr99 group was barely detected in both *VDJ-Cγ* and *VDJ-Cα* clones of NALT memory B cells (see Table I and Fig. 2 C and D). Thus, the low frequency of memory B cells together with the difference in genetics between NALT GC and memory B cells suggest that high affinity B cells generated in NALT GC could not be retained in NALT as a memory population.

We observed that the primary and secondary i.n. challenge with NP-CG caused secretion of a large amount of high affinity anti-NP IgA antibodies in nasal wash (data not shown). This led us to speculate that the newly differentiated memory B cells in NALT could promptly emigrate from the tissue and home back to reside underneath the epithelial cell layer of NALT, as observed previously in human NALT (41).

Since NALT preferentially drain to PCLNs (26, 27), we speculated that memory B cells generated in NALT could emigrate into the draining PCLNs through the lymphatic system and then to thoratic duct that joins the systemic circulation (42). As shown in Fig. 1 C, NIP binding/λ^+ GC B cells appeared in the PCLNs at day 9 and reached a plateau at days 11 to 15 after immunization, 4 d behind the response in NALT. This is in agreement with the view that NALT is the primary inductive site upon i.n. immunization (26–29). The frequency of GC B cells in PCLNs was $\sim$1–2 $\times$ 10^{-4} PCLN cells, 10 times below the level observed in NALT. The frequency of NIP-binding/λ^+/IgG2b$^+$ GC B cells that were the dominant subclass of IgG in the response was five times more than IgA$^+$ GC B cells throughout the reaction.

Fig. 1 D shows that NIP-binding B cells with memory phenotype transiently appeared in PCLNs, and peaked at day 11 after immunization at a frequency comparable to that of GC B cells. We observed that PCLNs consist of 2–5 $\times$ 10^6 cells in immunized mice, $\sim$10 times higher than NALT. Therefore, assuming that PCLN GC produce memory B cells at a similar rate to that observed for splenic GCs (see above and references 12 and 19), memory B cells derived from PCLN GC would amount to 100 cells per mouse at most. This would represent $\sim$20% of the estimated number of PCLN memory B cells (based on the FACS® data in Fig. 1 D). Notably, the frequency of IgA$^+$ memory B cells was comparable with that of IgG$^+$ memory B cells throughout the immune response (Fig. 1 D), and the frequency was 10 times higher than the expected value based on the frequency of IgA$^+$ PCLN GC B cells. Therefore, taking into account the low frequency of NALT memory B cells throughout the response, it is conceivable that IgA$^+$ memory B cells generated in NALT emigrate into the draining PCLNs (also see below).

High Affinity B Cells Are Enriched Exclusively in the IgA Memory Compartment in PCLNs. We purified NIP-binding/λ^+/B220$^+$/CD38^{dull} GC and NIP-binding/λ^+/B220$^+$/CD38$^+$ memory B cells from pooled PCLNs (n = 20–30) by FACS® (see Materials and Methods) and conducted PCR to amplify *VDJ-Cγ* and *VDJ-Cα* clones. As shown in Table I and Fig. 2 E, the *VDJ-Cγ* clones isolated from PCLN GC B cells transiently accumulated the Leu33 replacement and had increased numbers of mutations by day 15 after immunization. To our surprise, the *VDJ-Cγ* clones isolated from B cells with memory phenotype in PCLNs did not carry the Leu33 replacement, nor did they have an increased average number of mutations from days 11 to 21 after immunization (Fig. 2 G). Thus, it appears that IgG$^+$ B cells selected by antigen in GC reactions of PCLNs (Fig. 2 E) and NALT (Fig. 2 A) were largely missing from the IgG memory compartment of PCLNs.

Unlike the *VDJ-Cγ* clones, the *VDJ-Cα* clones isolated from PCLN GC B cells neither increased in average number of mutations nor accumulated the Leu33 replacement from days 11 to 15 after immunization (Fig. 2 F and Table I). However, the *VDJ-Cα* clones of memory B cells in PCLNs increased the average number of somatic mutations, accompanying accumulation of the affinity-enhancing Leu33 replacement at high frequency at days 13 and 15 after immunization (P = 0.0015 and P = 0.0173, respectively; Fig. 2 H and Table I). Like the *VDJ-Cγ* clones isolated from NALT GC B cells at day 11 after immunization, the *VDJ-Cα* clones of memory B cells in PCLNs at days 13 and 15 after immunization consisted largely of the *V186.2* genes joined to *DFL16.1* and J_H2 that carries Tyr99 (>80%, Table I), significantly different from the *VDJ-Cγ* clones of memory B cells in PCLNs ($P < 0.0261$, Table I). These results suggest that high affinity B cells are preferentially enriched in the IgA$^+$ memory compartment with time after i.n. immunization with NP-CG. In contrast, the NP-specific IgG$^+$ memory compartment is hardly occupied by high affinity B cells, despite the fact that CSR and antigen-driven selection were operated equally well in both the IgG$^+$ and IgA$^+$ GC compartments.

I.N. Immunization Followed by Intraperitoneal Challenge Causes Systemic Immune Response with High Affinity IgA. In agreement with the selective development of high-affinity IgA memory B cells in PCLNs described previously, we observed remarkable IgA affinity maturation in nasal secretions after primary and secondary i.n. inoculation with NP-CG and CT (data not shown). However, we could not analyze affinity maturation in anti-NP IgG antibodies because these antibodies were barely detected in nasal secretions (data not shown).

Therefore, to examine affinity maturation in the secondary response, we challenged C57BL/6 mice intraperitoneally with 20 μg of NP-CG, 5 wk after i.n. inoculation with NP-CG and CT. 7 d after the secondary challenge, the number of NP-binding/λ_1^+ ASCs in the spleen and bone marrow and the amount of anti-NP antibodies in the sera were determined by ELISPOT and ELISA, respectively. As shown in Fig. 3 A, the secondary intraperitoneal

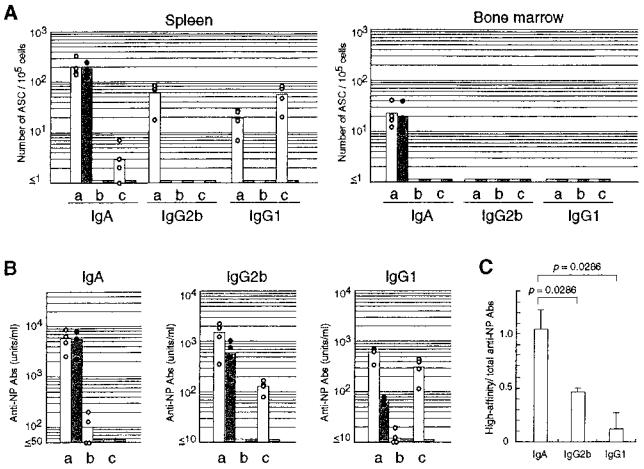

Figure 3. Dominance of high affinity IgA in the secondary response after i.n. immunization. C57BL/6 mice were primed i.n. with 2 μg of NP-CG and CT, followed by intraperitoneal challenge with 20 μg of either NP-CG (a) or CG (c) 5 wk later. As a control, mice were i.n. immunized with 2 μg of CG plus CT, followed by intraperitoneal challenge with NP-CG (b). 7 d after the intraperitoneal challenge, immune serum, spleen, and bone marrow were obtained from individual mice ($n = 4$). All data are representative of three independent experiments. (A) The numbers of total (○) and high affinity (●) NP-binding/λ_1^+ ASCs with IgA, IgG2b, and IgG1 subclasses were determined by ELISPOT. Columns represent the average number of total (white columns) and high affinity ASCs (black columns). (B) Total (○) and high affinity (●) NP-specific antibody titers of IgA, IgG2b, and IgG1 subclass in serum from individual mice ($n = 4$) were determined by ELISA. (C) Isotype-specific serum antibody affinity maturation was estimated for the individual mice ($n = 4$) shown in group a of B by dividing the high affinity NP-specific antibody titer by the total NP-specific antibody titer. Serum affinity maturation of NP-specific antibodies between IgA and IgG2b or IgG1 was statistically evaluated by the Mann-Whitney nonparametric tests (two-tailed).

challenge caused a substantial increase in the number of NP-binding/λ_1^+/IgA$^+$ ASCs in the spleen and bone marrow. NP-binding/λ_1^+/IgG2b$^+$ ASCs were also increased in the spleen of mice primed i.n. with NP-CG and CT, but not in control mice primed with CG and CT. >90% of NP-binding/λ_1^+/IgA$^+$ ASCs secreted high affinity antibodies, whereas NP-binding/λ_1^+/IgG2b$^+$ ASCs did not.

In agreement with the ELISPOT results, the secondary challenge with NP-CG resulted in increased levels of anti-NP IgA and IgG2b antibodies in the sera of mice primed i.n. with NP-CG and CT, ~100 and 10 times above the level of mice primed with CG and CT, respectively (Fig. 3 B). Again, IgA antibodies were comprised largely of high affinity antibodies (>90%), whereas the proportion of high affinity antibodies was less in IgG2b (46% on the average; Fig. 3 C, $P = 0.0286$). A significant difference in the affinity maturation between IgA and IgG2b serum antibodies was reproducible (data not shown).

As shown in Fig. 3 A and B, the secondary challenge with NP-CG did not cause any significant secondary response with IgG1 ASCs and IgG1 antibodies (Fig. 3 C, $P = 0.0286$) in the mice primed i.n. with NP-CG and CT, suggesting that the primary i.n. inoculation with NP-CG and CT does not efficiently develop IgG1 memory B cells (see Table I).

Migration of Memory B Cells into Nonmucosal Lymphoid Tissues via the Systemic Circulation. To examine whether high affinity IgA memory B cells migrate into nonmucosal tissues through the systemic circulation as predicted above, we obtained splenocytes from the pooled spleens ($n = 5$–6) of C57BL/6 mice that had been primed i.n. with CT and either NP-CG or CG 7 wk previously. These cells were transferred into RAG-1$^{-/-}$ mice on a C57BL/6 background, followed by challenge with soluble NP-CG. 10 d later, we estimated anti-NP antibody levels in serum by ELISA. As shown in Fig. 4 A, the RAG-1$^{-/-}$ mice reconstituted with NP-CG–primed splenocytes produced a significant amount of anti-NP antibodies of the IgA subclass after immunization with NP-CG, ~10-fold above the level of RAG-1$^{-/-}$ mice reconstituted with CG-primed cells. In contrast, the level of anti-NP IgG1$^+$ and IgG2b$^+$ antibodies in RAG-1$^{-/-}$ mice reconstituted with NP-CG–primed splenocytes was less than twofold above the level of mice reconstituted with CG-primed cells. In addition, anti-NP IgA antibody was dominated by high affinity antibodies (70%), whereas high affinity antibodies were less frequent among IgG1$^+$ and IgG2b$^+$ antibodies compared with the level of IgA antibodies ($P = 0.0571$ and $P = 0.0286$, respectively; Fig. 4 B).

Taken together, these results demonstrate that B cell activation in NALT upon stimulation with NP-CG and CT resulted in a clonal dominance of high affinity B cells in the IgA$^+$ memory compartment, although antigen-driven se-

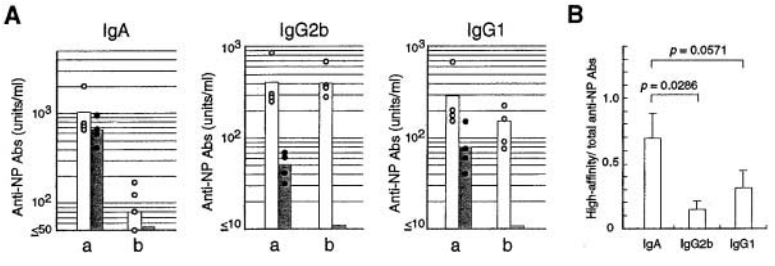

Figure 4. High affinity IgA memory cells generated in NALT migrate into nonmucosal lymphoid tissues such as spleen. C57BL/6 were immunized i.n. with 2 μg of CT and 2 μg of either NP-CG (a) or CG (b). 4 wk later, single cell suspensions were prepared from pooled spleens ($n = 4$) and transferred into RAG-1$^{-/-}$ mice on a C57BL/6 background by intravenous injection (6×10^7 cells per recipient). 12–24 h after the transfer, the reconstituted RAG-1$^{-/-}$ mice were immunized intraperitoneal with 50 μg of NP-CG. All data are representative of three independent experiments. (A) 7 d later, the levels of NP-specific antibodies (○) and high affinity NP-specific antibodies (●) of IgA, IgG2b, and IgG1 subclasses in individual sera ($n = 4$) were determined by ELISA. White and black columns represent the mean titer of total and high affinity anti-NP antibodies, respectively. (B) Isotype-specific serum antibody affinity maturation was estimated for the individual mice ($n = 4$) shown in group (a) of A by dividing the high affinity NP-specific antibody titer by the total NP-specific antibody titer. Serum affinity maturation of NP-specific antibodies between IgA and IgG2b or IgG1 was statistically evaluated by the Mann-Whitney nonparametric tests (two-tailed).

lection appeared to operate equally well in the IgG^+ and IgA^+ GC compartments in NALT.

IgA^+ memory B cells were barely detected in NALT but transiently appeared in PCLNs at a level similar to that of IgA^+ GC B cells, 4 d behind the peak of GC response in NALT. The rearranged *V186.2* genes from IgA^+ memory B cells in PCLN exhibited indications of antigen-driven selection comparable in several respects to the features of *V186.2* genes in the IgA^+ GC B cells in NALT. However, IgA^+ GC B cells in PCLNs had a low number of mutations throughout the immune response, with no association with the affinity-enhancing Leu33 mutation (Table I and Fig. 2 F). The differences in *VDJ-Cα* clonotypes between GC B cells and memory B cells in PCLNs support the view that IgA^+ memory B cells in PCLNs represent the progeny of IgA^+ GC B cells generated in NALT but not in PCLNs.

Although NP-specific $IgG2b^+$ GC B cells dominated over the IgA^+ GC B cells in NALT and PCLNs after immunization, the number of $IgG2b^+$ and IgA^+ memory B cells was almost comparable throughout the immune response in PCLNs. $IgG2b^+$ GC B cells accumulated mutations with indications of affinity maturation during the peak response in NALT and PCLNs, while such features were hardly observed in $IgG2b^+$ memory B cells in PCLNs. The correlation of high affinity IgA dominance with a lack of high affinity IgG in PCLN memory B cells (Table I and Fig. 2 G and H) led us to speculate that preferential enrichment of high affinity IgA^+ memory cells might be a result of enhanced CSR at *Cγ* during sequential CSR from *Cμ* to *Cα* via *Cγ* in high affinity IgG^+ GC B cells in NALT and PCLNs.

Sequential CSR from *Cμ* to *Cα* via *Cγ* was detected in the development of IgA-producing cells in vitro in the presence of TGF-β (7, 47), in which sequential CSR from *Cμ* to *Cα* via *Cγ*2b appeared to be dominant (7). In addition, in mutant mice depleted of IgA, TGF-β, and TGF-β receptor type II, the deficiency in the development of IgA-expressing plasma cells is associated with enhancement of IgG expression in serum, mucosal secretions, and Peyer's patches (9, 48, 49), compatible with the notion that sequential CSR could be frequent in vivo. B cell function mediated by B cell receptor depends on antibody avidity, which is associated with the number and affinity of surface Igs (50, 51). High affinity B cells may gain more potent APC function (50, 51), which may, in turn, result in frequent contact with Th cells. Several in vitro studies have emphasized the significance of CD40 signaling in IgA CSR (8, 47, 52). Therefore, cognate interaction between Th cells not only through B cell receptor but, together with coreceptors, may deliver the signal(s) for chromosomal accessibility at the *Ig* locus that are essential for sequential CSR from *Cγ* to *Cα* in the mucosal environment. However, we could not exclude the possibility at present that the differentiation of high affinity IgG GC B cells into ASCs and memory cells is impaired in NALT. Further analysis is needed to clarify this issue.

This study demonstrates that a GC reaction is rapidly induced in NALT after i.n. inoculation with a minute amount of NP-CG and CT. However, it remains unknown whether mucosal GCs in NALT are structurally and functionally compatible with GCs formed in the spleen and peripheral LNs. We observed that NP-specific B cells indicative of affinity maturation were selected among IgA^+ B cells earlier than among IgG^+ B cells in NALT GC after immunization (Fig. 2 A and B). In taking account of possible isotype-specific signaling events (53), it is worthwhile to analyze whether the structural differences in the transmembrane and cytoplasmic domains of IgA and IgG might be responsible for the isotype-dependent selection in NALT GC.

GC B cells in the spleen continuously accumulate somatic mutations over long periods after intraperitoneal immunization with NP-CG in alum (19), whereas NALT GC B cells appeared to undergo transient accumulation of mutations. Likewise, IgA^+ GC B cells with indications of affinity maturation increased in number in NALT at day 9 after immunization, whereas these cells became undetectable from days 9 to 11 after immunization (Fig. 2 A and Table I). Interestingly, however, IgA^+ GC B cells with indications of affinity maturation reappeared later at day 13 after immunization (Fig. 2 A and Table I). It would be worthwhile to analyze whether or not the reappearance reflects sequential CSR from *Cμ* to *Cα* via *Cγ* in high affinity IgG B cells. The transient nature of enrichment of high affinity variants in GC may imply that the high affinity GC B cells immediately differentiated into long-term ASCs and/or memory cells and quickly left GC. Consistent with this possibility, we observed that high affinity IgA antibodies started to appear in nasal secretions at day 11 after primary immunization and accounted for 40% of total anti-NP IgA antibodies at day 21 immunization (data not shown).

Previous reports suggest that memory B cells reach a plateau after the peak response of GC and retain this level for long periods in the spleen after intraperitoneal immunization with NP-CG (12, 19). However, it appears that memory B cells differentiated from NALT GC B cells promptly migrate into the draining LNs through the lymphatic system and then further migrate into the general circulation, rather than being retained in these lymphoid tissues for a longer period. A fraction of these memory B cells at least may reside in the spleen and nasal mucosa. The less efficient retention of memory B cells in NALTs and PCLNs may in part be related to their histological organization, being distinct from the spleen where memory B cells often localize in the marginal zone (10, 54).

In summary, this study sheds light on the GC reaction responsible for generating mucosal memory B cells. Our genetic analysis suggests that NALTs preferentially select high affinity IgA^+ B cells in the memory compartment. This mechanism has the great advantage of facilitating immunity with noninflammatory, high affinity secretory IgA antibodies with far greater efficiency than that of other subclasses of antibodies. Whether this system is unique to NALTs or common to other mucosal lymphoid tissues remains to be elucidated.

We are grateful to Drs. T. Tsubata for discussions, G.H. Kelso for sharing unpublished data, P.A. Koni for critical reviewing, T. Azuma and K. Furukawa for the reagents, and Ms. Y. Nakano for technical help.

This work was supported by grants from the Agency of Technology and Science of the Japanese government to T. Takemori, the Ministry of Education, Science, Sport, and Culture to T. Takemori and C. Kanno, and the Japan Food Industry Center to C. Kanno.

Submitted: 27 March 2001
Accepted: 10 September 2001

References

1. Neutra, M.R., E. Pringault, and J.P. Kraehenbuhl. 1996. Antigen sampling across epithelial barriers and induction of mucosal immune responses. *Annu. Rev. Immunol.* 14:275–300.
2. Neutra, M.R. 1999. M cells in antigen sampling in mucosal tissues. *Curr. Top. Microbiol. Immunol.* 236:17–32.
3. Brandtzaeg, P., E.S. Baekkevold, I.N. Farstad, F.L. Jahnsen, F.E. Johansen, E.M. Nilsen, and T. Yamanaka. 1999. Regional specialization in the mucosal immune system: what happens in the microcompartments? *Immunol. Today.* 20: 141–151.
4. Corthesy, B., and J.P. Kraehenbuhl. 1999. Antibody-mediated protection of mucosal surfaces. *Curr. Top. Microbiol. Immunol.* 236:93–111.
5. Weinstein, P.D., and J.J. Cebra. 1991. The preference for switching to IgA expression by Peyer's patch germinal center B cells is likely due to the intrinsic influence of their microenvironment. *J. Immunol.* 147:4126–4135.
6. Defrance, T., B. Vanbervliet, F. Briere, I. Durand, F. Rousset, and J. Banchereau. 1992. Interleukin 10 and transforming growth factor β cooperate to induce anti-CD40-activated naive human B cells to secrete immunoglobulin A. *J. Exp. Med.* 175:671–682.
7. Iwasato, T., H. Arakawa, A. Shimizu, T. Honjo, and H. Yamagishi. 1992. Biased distribution of recombination sites within S regions upon immunoglobulin class switch recombination induced by transforming growth factor β and lipopolysaccharide. *J. Exp. Med.* 175:1539–1546.
8. McIntyre, T.M., M.R. Kehry, and C.M. Snapper. 1995. Novel in vitro model for high-rate IgA class switching. *J. Immunol.* 154:3156–3161.
9. Cazac, B.B., and J. Roes. 2000. TGF-β receptor controls B cell responsiveness and induction of IgA in vivo. *Immunity.* 13:443–451.
10. Liu, Y.J., J. Zhang, P.J. Lane, E.Y. Chan, and I.C. MacLennan. 1991. Sites of specific B cell activation in primary and secondary responses to T cell-dependent and T cell-independent antigens. *Eur. J. Immunol.* 21:2951–2962.
11. Kelsoe, G. 1996. Life and death in germinal centers (redux). *Immunity.* 4:107–111.
12. Ridderstad, A., and D.M. Tarlinton. 1998. Kinetics of establishing the memory B cell population as revealed by CD38 expression. *J. Immunol.* 160:4688–4695.
13. Bachmann, M.F., B. Odermatt, H. Hengartner, and R.M. Zinkernagel. 1996. Induction of long-lived germinal centers associated with persisting antigen after viral infection. *J. Exp. Med.* 183:2259–2269.
14. Schittek, B., and K. Rajewsky. 1990. Maintenance of B-cell memory by long-lived cells generated from proliferating precursors. *Nature.* 346:749–751.
15. Gray, D., P. Dullforce, and S. Jainandunsing. 1994. Memory B cell development but not germinal center formation is impaired by in vivo blockade of CD40–CD40 ligand interaction. *J. Exp. Med.* 180:141–155.
16. Manz, R.A., A. Thiel, and A. Radbruch. 1997. Lifetime of plasma cells in the bone marrow. *Nature.* 388:133–134.
17. Smith, K.G., A. Light, G.J. Nossal, and D.M. Tarlinton. 1997. The extent of affinity maturation differs between the memory and antibody-forming cell compartments in the primary immune response. *EMBO J.* 16:2996–3006.
18. Slifka, M.K., R. Antia, J.K. Whitmire, and R. Ahmed. 1998. Humoral immunity due to long-lived plasma cells. *Immunity.* 8:363–372.
19. Takahashi, Y., H. Ohta, and T. Takemori. 2001. Fas is required for clonal selection in germinal centers and the subsequent establishment of the memory B cell repertoire. *Immunity.* 14:181–192.
20. Berek, C., A. Berger, and M. Apel. 1991. Maturation of the immune response in germinal centers. *Cell.* 67:1121–1129.
21. Jacob, J., G. Kelsoe, K. Rajewsky, and U. Weiss. 1991. Intraclonal generation of antibody mutants in germinal centres. *Nature.* 354:389–392.
22. Hande, S., E. Notidis, and T. Manser. 1998. Bcl-2 obstructs negative selection of autoreactive, hypermutated antibody V regions during memory B cell development. *Immunity.* 8:189–198.
23. Pulendran, B., R. van Driel, and G.J. Nossal. 1997. Immunological tolerance in germinal centres. *Immunol. Today.* 18: 27–32.
24. Liu, Y.J., F. Malisan, O. de Bouteiller, C. Guret, S. Lebecque, J. Banchereau, F.C. Mills, E.E. Max, and H. Martinez-Valdez. 1996. Within germinal centers, isotype switching of immunoglobulin genes occurs after the onset of somatic mutation. *Immunity.* 4:241–250.
25. Kuppers, R., M. Zhao, M.L. Hansmann, and K. Rajewsky. 1993. Tracing B cell development in human germinal centres by molecular analysis of single cells picked from histological sections. *EMBO J.* 12:4955–4967.
26. Kuper, C.F., P.J. Koornstra, D.M. Hameleers, J. Biewenga, B.J. Spit, A.M. Duijvestijn, P.J. van Breda Vriesman, and T. Sminia. 1992. The role of nasopharyngeal lymphoid tissue. *Immunol. Today.* 13:219–224.
27. Wu, H.Y., and M.W. Russell. 1997. Nasal lymphoid tissue, intranasal immunization, and compartmentalization of the common mucosal immune system. *Immunol. Res.* 16:187–201.
28. Asanuma, H., A.H. Thompson, T. Iwasaki, Y. Sato, Y. Inaba, C. Aizawa, T. Kurata, and S. Tamura. 1997. Isolation and characterization of mouse nasal-associated lymphoid tissue. *J. Immunol. Methods.* 202:123–131.
29. Wu, H.Y., H.H. Nguyen, and M.W. Russell. 1997. Nasal lymphoid tissue (NALT) as a mucosal immune inductive site. *Scand. J. Immunol.* 46:506–513.
30. Bothwell, A.L., M. Paskind, M. Reth, T. Imanishi-Kari, K. Rajewsky, and D. Baltimore. 1981. Heavy chain variable region contribution to the NPb family of antibodies: somatic mutation evident in a γ 2a variable region. *Cell.* 24:625–637.
31. Cumano, A., and K. Rajewsky. 1985. Structure of primary anti-(4-hydroxy-3-nitrophenyl)acetyl (NP) antibodies in normal and idiotypically suppressed C57BL/6 mice. *Eur. J. Immunol.* 15:512–520.
32. Weiss, U., and K. Rajewsky. 1990. The repertoire of somatic

antibody mutants accumulating in the memory compartment after primary immunization is restricted through affinity maturation and mirrors that expressed in the secondary response. *J. Exp. Med.* 172:1681–1689.
33. McHeyzer-Williams, M.G., M.J. McLean, P.A. Lalor, and G.J. Nossal. 1993. Antigen-driven B cell differentiation in vivo. *J. Exp. Med.* 178:295–307.
34. Kimoto, H., H. Nagaoka, Y. Adachi, T. Mizuochi, T. Azuma, T. Yagi, T. Sata, S. Yonehara, Y. Tsunetsugu-Yokota, M. Taniguchi, and T. Takemori. 1997. Accumulation of somatic hypermutation and antigen-driven selection in rapidly cycling surface Ig^+ germinal center (GC) B cells which occupy GC at a high frequency during the primary anti-hapten response in mice. *Eur. J. Immunol.* 27:268–279.
35. Takahashi, Y., P.R. Dutta, D.M. Cerasoli, and G. Kelsoe. 1998. In situ studies of the primary immune response to (4-hydroxy-3-nitrophenyl)acetyl. V. Affinity maturation develops in two stages of clonal selection. *J. Exp. Med.* 187:885–895.
36. Wu, H.Y., E.B. Nikolova, K.W. Beagley, J.H. Eldridge, and M.W. Russell. 1997. Development of antibody-secreting cells and antigen-specific T cells in cervical lymph nodes after intranasal immunization. *Infect. Immun.* 65:227–235.
37. Oliver, A.M., F. Martin, and J.F. Kearney. 1997. Mouse CD38 is down-regulated on germinal center B cells and mature plasma cells. *J. Immunol.* 158:1108–1115.
38. Reth, M., G.J. Hammerling, and K. Rajewsky. 1978. Analysis of the repertoire of anti-NP antibodies in C57BL/6 mice by cell fusion. I. Characterization of antibody families in the primary and hyperimmune response. *Eur. J. Immunol.* 8:393–400.
39. Smith, K.G., T.D. Hewitson, G.J. Nossal, and D.M. Tarlinton. 1996. The phenotype and fate of the antibody-forming cells of the splenic foci. *Eur. J. Immunol.* 26:444–448.
40. Rose, M.L., M.S. Birbeck, V.J. Wallis, J.A. Forrester, and A.J. Davies. 1980. Peanut lectin binding properties of germinal centres of mouse lymphoid tissue. *Nature.* 284:364–366.
41. Liu, Y.J., C. Barthelemy, O. de Bouteiller, C. Arpin, I. Durand, and J. Banchereau. 1995. Memory B cells from human tonsils colonize mucosal epithelium and directly present antigen to T cells by rapid up-regulation of B7-1 and B7-2. *Immunity.* 2:239–248.
42. Brandtzaeg, P., I.N. Farstad, and G. Haraldsen. 1999. Regional specialization in the mucosal immune system: primed cells do not always home along the same track. *Immunol. Today.* 20:267–277.
43. Bothwell, A.L., M. Paskind, M. Reth, T. Imanishi-Kari, K. Rajewsky, and D. Baltimore. 1982. Somatic variants of murine immunoglobulin λ light chains. *Nature.* 298:380–382.
44. Furukawa, K., A. Akasako-Furukawa, H. Shirai, H. Nakamura, and T. Azuma. 1999. Junctional amino acids determine the maturation pathway of an antibody. *Immunity.* 11: 329–338.
45. Maizels, N., and A. Bothwell. 1985. The T cell-independent immune response to the hapten NP uses a large repertoire of heavy chain genes. *Cell.* 43:715–720.
46. Allen, D., T. Simon, F. Sablitzky, K. Rajewsky, and A. Cumano. 1988. Antibody engineering for the analysis of affinity maturation of an anti-hapten response. *EMBO J.* 7:1995–2001.
47. Zan, H., A. Cerutti, P. Dramitinos, A. Schaffer, and P. Casali. 1998. CD40 engagement triggers switching to IgA1 and IgA2 in human B cells through induction of endogenous TGF-β: evidence for TGF-β but not IL-10-dependent direct S mu→S α and sequential S mu→S γ, S γ→S α DNA recombination. *J. Immunol.* 161:5217–5225.
48. Harriman, G.R., M. Bogue, P. Rogers, M. Finegold, S. Pacheco, A. Bradley, Y. Zhang, and I.N. Mbawuike. 1999. Targeted deletion of the IgA constant region in mice leads to IgA deficiency with alterations in expression of other Ig isotypes. *J. Immunol.* 162:2521–2529.
49. van Ginkel, F.W., S.M. Wahl, J.F. Kearney, M.N. Kweon, K. Fujihashi, P.D. Burrows, H. Kiyono, and J.R. McGhee. 1999. Partial IgA-deficiency with increased Th2-type cytokines in TGF-β1 knockout mice. *J. Immunol.* 163:1951–1957.
50. Batista, F.D., and M.S. Neuberger. 1998. Affinity dependence of the B cell response to antigen: a threshold, a ceiling, and the importance of off-rate. *Immunity.* 8:751–759.
51. Batista, F.D., and M.S. Neuberger. 2000. B cells extract and present immobilized antigen: implications for affinity discrimination. *EMBO J.* 19:513–520.
52. Deenick, E.K., J. Hasbold, and P.D. Hodgkin. 1999. Switching to IgG3, IgG2b, and IgA is division linked and independent, revealing a stochastic framework for describing differentiation. *J. Immunol.* 163:4707–4714.
53. Pogue, S.L., and C.C. Goodnow. 2000. Gene dose-dependent maturation and receptor editing of B cells expressing immunoglobulin (Ig)G1 or IgM/IgG1 tail antigen receptors. *J. Exp. Med.* 191:1031–1044.
54. Dunn-Walters, D.K., P.G. Isaacson, and J. Spencer. 1995. Analysis of mutations in immunoglobulin heavy chain variable region genes of microdissected marginal zone (MGZ) B cells suggests that the MGZ of human spleen is a reservoir of memory B cells. *J. Exp. Med.* 182:559–566.